processes

MDPI

Article

Anammox-Based Processes for Mature Leachate Treatment in SBR: A Modelling Study

Anna Lanzetta [1], Davide Mattioli [2], Francesco Di Capua [1,3], Gianpaolo Sabia [2], Luigi Petta [2], Giovanni Esposito [1], Gianni Andreottola [4], Giovanni Gatti [5], Willy Merz [6] and Michela Langone [7,*]

1 Department of Civil, Architectural and Environmental Engineering, University of Naples Federico II, Via Claudio 21, 80125 Naples, Italy; anna.lanzetta@unina.it (A.L.); francesco.dicapua@poliba.it (F.D.C.); gioespos@unina.it (G.E.)
2 Laboratory Technologies for the Efficient Use and Management of Water and Wastewater, Italian National Agency for New Technologies, Energy and Sustainable Economic Development (ENEA), Via M.M. Sole 4, 40129 Bologna, Italy; davide.mattioli@enea.it (D.M.); gianpaolo.sabia@enea.it (G.S.); luigi.petta@enea.it (L.P.)
3 Department of Civil, Environmental, Land, Building Engineering and Chemistry, Polytechnic University of Bari, Via E. Orabona 4, 70125 Bari, Italy
4 Department of Civil, Environmental and Mechanical Engineering, University of Trento, 38123 Trento, Italy; gianni.andreottola@unitn.it
5 ADEP, Agenzia per la Depurazione (Wastewater Treatment Agency)-Serv. Gestione degli impianti, Autonomous Province of Trento, Via Gilli 3, 38121 Trento, Italy; giovanni.gatti@provincia.tn.it
6 APOP, Ag. Prov.le per le Opere Pubbliche (Provincial Agency for Public Works)-Serv. Opere Ambientali Province of Trento, Via Mantova 67, 38121 Trento, Italy; willy.merz@provincia.tn.it
7 Laboratory Technologies for the Efficient Use and Management of Water and Wastewater, Italian National Agency for New Technologies, Energy and Sustainable Economic Development (ENEA), Via Anguillarese, 301, 00123 Rome, Italy
* Correspondence: michela.langone@enea.it

Abstract: Mature landfill leachates are characterized by high levels of ammoniacal nitrogen which must be reduced for discharge in the sewer system and further treatment in municipal wastewater treatment plants. The use of anammox-based processes can allow for an efficient treatment of ammonium-rich leachates. In this work, two real scale sequencing batch reactors (SBRs), designed to initially perform partial nitritation/anammox (PN/A) and simultaneous partial nitrification and denitrification (SPND) for the treatment of ammonium-rich urban landfill leachate, were modelled using BioWin 6.0 in order to enable plant-wide modelling and optimizing. The constructed models were calibrated and validated using data from long- and short-term (one cycle) SBR operation and fit well to the main physical-chemical parameters (i.e., ammonium, nitrite and nitrate concentrations) measured during short-term (one cycle) operations. Despite the different strategies in terms of dissolved oxygen (DO) concentrations and aeration and mixing patterns applied for SBR operation, the models allowed for understanding that in both reactors the PN/A process was shown as the main contributor to nitrogen removal when the availability of organic carbon was low. Indeed, in both SBRs, the activity of nitrite oxidizing bacteria was inhibited due to high levels of free ammonia, whereas anammox bacteria were active due to the simultaneous presence of ammonium and nitrite and their ability to recover from DO inhibition. Increasing the external carbon addition, a prompt decrease of the anammox biomass was observed, with SPND becoming the main nitrogen removal mechanism. Models were also applied to estimate the production rates of nitrous oxide by aerobic ammonia oxidizing bacteria and heterotrophic denitrifiers. The models were found to be a robust tool for understanding the effects of different operating conditions (i.e, temperature, cycle phases, DO concentration, external carbon addition) on the nitrogen removal performances of the two reactors, assessing the contribution of the different bacterial groups involved.

Keywords: anaerobic ammonium oxidation; denitrification; leachate pre-treatment; nitrogen removal; partial nitritation; sequencing batch reactor; WWTP modelling

Citation: Lanzetta, A.; Mattioli, D.; Di Capua, F.; Sabia, G.; Petta, L.; Esposito, G.; Andreottola, G.; Gatti, G.; Merz, W.; Langone, M. Anammox-Based Processes for Mature Leachate Treatment in SBR: A Modelling Study. *Processes* **2021**, *9*, 1443. https://doi.org/10.3390/pr9081443

Academic Editors: Albert Magrí and Tommaso Lotti

Received: 17 June 2021
Accepted: 16 August 2021
Published: 19 August 2021

1. Introduction

Mature landfill leachates are heterogenous liquid streams generally characterized by a low content of biodegradable organic carbon and high concentrations of organic and inorganic contaminants [1]. Among these, total ammonium nitrogen (TAN) can reach concentrations of several thousands of mg L^{-1} [2,3], posing a serious challenge to downstream wastewater treatments. As a result, ammonium-rich landfill leachate must undergo a pretreatment for nitrogen removal before entering the municipal wastewater treatment plant (WWTP). Physical-chemical methods for nitrogen removal such as ammonia stripping and chemical precipitation require a large amount of chemicals, i.e., sulfuric, hydrochloric or phosphoric acids, for NH_3 absorption in stripping columns [4] or magnesium and phosphate salts for TAN precipitation as struvite [5], leading to high operational costs. Biological processes are less expensive and result in the efficient removal of both nitrogen and organic carbon. However, treatment of ammonium-rich landfill leachate by conventional nitrification and denitrification processes requires organic carbon supplementation to satisfy carbon demand for denitrification, as well as a high oxygen supply, resulting in reduced economic advantages and potential secondary pollution [6]. For wastewaters with low carbon-to-nitrogen ratio (C/N), anaerobic ammonium oxidation (anammox) coupled with nitritation process (i.e., ammonium oxidation to nitrite) is regarded as a more sustainable and cost-effective biological process than conventional nitrification and denitrification [7], due to its lower demand for aeration and organic carbon.

The anammox process implies ammonium (NH_4^+) oxidation coupled to nitrite (NO_2^-) reduction to nitrogen gas (N_2) by autotrophic anaerobic ammonium oxidizing bacteria (AAO) (1). Thus, for the treatment of ammonium-contaminated wastewaters, the anammox process needs to be enabled by the ammonium conversion to NO_2^- through partial nitritation (PN) carried out by ammonium oxidizing bacteria (AOB) (2), while NO_2^- oxidation to nitrate (NO_3^-) by nitrite oxidizing bacteria (NOB) must be inhibited, being a parasite process consuming the electron acceptor required for anammox bacteria.

$$NH_4^+ + 1.32\ NO_2^- + 0.066\ HCO_3^- + 0.13\ H^+ \rightarrow 1.02\ N_2 + 0.26\ NO_3^- + 2.03\ H_2O + 0.066\ CH_2O_{0.5}N_{0.15} \quad (1)$$

$$NH_4^+ + 0.79\ O_2 + 1.14\ HCO_3^- \rightarrow 0.010\ C_5H_7NO_2 + 0.43\ NH_4^+ + 0.56\ NO_2^- + 1.09\ CO_2 + 1.68\ H_2O \quad (2)$$

NOB inhibition can be achieved by operating the bioreactors at high pH (>7.5) and temperatures (>25 °C) [8,9], low sludge retention time (SRT) (<4 days) [10], low dissolved oxygen (DO) concentration (<2 mg L^{-1}) [11] and by maintaining the concentrations of free ammonia (FA) and free nitrous acid (FNA) within certain ranges being inhibitory for NOB and tolerable by AOB [12,13].

The PN/anammox (PN/A) process can be successfully performed in a single sequencing batch reactor (SBR) under the alternation of aerobic and anoxic phases, which is controlled by monitoring specific parameters such as phase duration, pH, oxidation-reduction potential (ORP), SRT, DO level and nitrogen concentrations [14,15].

An alternative to the anammox process for the treatment of ammonium-contaminated streams is represented by simultaneous partial nitrification and denitrification (SPND) [10,16,17]. Similarly to the PN/A process, the SPND process requires the inhibition of NOB activity and results in lower oxygen and organic carbon consumption compared to conventional nitrification denitrification process [18].

Both PN/A and SPND guarantee significant advantages compared to conventional nitrification and denitrification in terms of energy consumption and operational costs. However, these processes are more sensitive to operational changes than conventional nitrogen removal, as they rely on the selection and maintenance of specific microbial communities. For instance, real-scale SBR commonly experience fluctuations of feeding and operational conditions due to seasonal variation of temperature and of carbon and nitrogen loadings, resulting in challenging reactor operation since they can lead to variations in microbial community composition, which should be monitored to maintain the reactor performance stable.

Due to the slow growth of the autotrophic bacteria involved, investigating nitrogen removal processes demands long and expensive experiments. Indeed, mathematical modelling represents an effective tool to predict reactor performance under varying input conditions and can help plant operators to avoid reactor failure and respect effluent standards. Moreover, mathematical modelling may allow to reduce costs and time for experiments and is useful for researchers and engineers to design, analyse and optimize wastewater treatments, especially when full-scale data are provided for model calibration and validation.

Although mathematical modelling of anammox-based processes has attained a degree of maturity in recent years [19], Baeten et al. [20] recommended to perform full scale model validation studies, in order to prevent system control problems and optimize biological removal.

The present study models the performances of two full-scale SBRs operated with the aim of achieving two different nitrogen removal bioprocesses, i.e., PN/A and SPND, for the treatment of mature landfill leachate contaminated by high concentrations of ammonium. By using the software BioWin, different operational conditions were simulated with the aim of investigating the related impacts on process performances and the contribution to nitrogen removal of the involved bacteria, i.e., AOB, NOB, AAO and ordinary heterotrophic bacteria (OHO). The two SBR models developed in this study were applied for optimizing the operational conditions of the leachate treatment plant under investigation.

2. Materials and Methods

2.1. Leachate Treatment Plant Description and Operation

The reference full-scale treatment plant is located in Lavis, Trento, Italy (Supplementary Material, Figure S1), and treats the leachate originating from the surrounding municipal solid waste landfills. The geographical origin of the leachate depends on rain seasonal regime, storage capacity of each landfill, leachate collection system and specific local management needs. During the monitoring campaign, the influent leachate was a mixture of streams coming from the different sections of each landfill.

Lavis landfill leachate treatment plant was originally designed as a chemical-biological plant for the removal of nitrogen and metals and has been in operation since 2012 to treat a maximum inflow capacity of 300 m^3 d^{-1}. The plant configuration consists of screens (1 mm), leachate storage tanks (510 m^3), organic carbon storage tanks (110 m^3), a chemical-physical section for heavy metals removal, a loading tank (30 m^3) and two parallel SBR units (each one with a maximum operating volume of 906 m^3) performing nitrogen removal through anammox-based processes, followed by a nitrifying/denitrifying membrane bioreactor (MBR) with an operating volume of 69.3 m^3.

Due to low metal concentrations in the influent leachate and relatively high nitrogen removal efficiency in the SBRs, both the chemical-physical section and MBR have never been put into operation.

Nevertheless, the envisaged and developed SBR treatment system implemented with DEMON® technology [21] to perform the PN/A process could not allow a stable nitrogen removal efficiency. Thus, since 2015, the two SBRs have been operated differently. One SBR (SBR_A) has been operated in a PN/A mode, with a different control logic than DEMON® technology, while the other reactor (SBR_B) has been operated in SPND mode. The treated leachate is then withdrawn, in accordance with the standards for discharge into municipal public sewers, to the municipal WWTP to undergo further biological treatments before final discharge into the Adige river. The schematic diagram of the leachate treatment plant is reported in Supplementary Material (Figure S2).

The SBR_A was inoculated with the PN/A biomass cultivated in the previous DEMON® process (micro-granules were present since the start-up), while activated sludge of the Lavis WWTP was used to inoculate the SBR_B. At the time of this study, the SBR_A was operated with an ammonium-nitrogen loading rate (NLR) of 0–0.069 kg N m^{-3} d^{-1} and an average exchange volume per cycle of approximately 29.7 m^3, resulting in a volume

exchange ratio of 3.3% and an average hydraulic retention time (HRT) of 15.2 days. The SBR_B was operated with a NLR of 0–0.050 kg N m^{-3} d^{-1}, an average exchange volume per cycle of approximately 21.5 m^3 and an average HRT of 20.5 days. Small micro-granules were observed also in the SBR_B at the time of this study.

Each SBR is equipped with a feed pump (3.7 kW), two 3.3 kW stirrers, and a sprinkling system for foam control. Both SBRs are covered to reduce heat loss and the aeration is performed by membrane-type fine bubble air diffusers (Aquastrip panels—ASCO POMPE SRL, Italy—and MESSNER Aeration Panel®—RMU RUDOLF MESSNER UMWELTTECHNIK AG, Germany—for SBR_A and SBR_B, respectively). The aeration unit is equipped with inverter technology compressors (Robuschi, Italy): one 14.2 kW compressor for SBR_A and two 13.6 kW compressors for SBR_B, respectively. Each SBR is further equipped with a telescopic decanter, controlled by water level, allowing the discharge from the upper part of the reactor after sludge sedimentation (the volume discharged per cycle is in the range of 2.5–7.0% of the reactor volume). During this study, the hydrocyclone (2.8 kW)—previously used operated with DEMON® technology to retain the anammox granules (heavier material) in the system under gravimetric forces while wasting the lighter portion of biomass—is only used in the SBR_A for separating heavy particles of material from lighter particles, without any actual biomass discharge. Both SBRs are controlled by a programmable logical controller and a supervisory control and data acquisition (SCADA) system as interface for the operator. The systems are equipped with online sensors to monitor and control the water level, air flow, temperature, pH and ORP.

During this study, a time-based control logic was applied to both SBRs by defining a fixed number of daily cycles and a fixed time for each process phase according to the efficiency observed in previous cycles. For a more effective nitrogen removal, one/two cycles per day were expected for both SBRs, each cycle typically lasting between 10 and 12 h. The cycle included an initial non-aerated feeding, which was time-controlled either (a) depending on the availability of leachate to be treated, (b) when the maximal fill level of the reactor was reached or (c) when a maximal TAN concentration was reached (e.g., 85 mg TAN·L^{-1}). The stirring unit was switched on during feeding and other process phases except the settling phase. The cycle comprised one or several aeration phases followed by one or several mixing phases to perform the PN/A process in SBR_A, and the SPND process in SBR_B. In SBR_A, an initial feeding phase of an external organic source (i.e., buttermilk) was sometimes provided, together with an additional mixing phase, in order to allow the consumption of residual nitrate or nitrite from the previous cycle by means of heterotrophic denitrification. In SBR_B, the feeding of an external organic source was always provided between each aeration and mixing phases to obtain better heterotrophic denitrification performances.

The aeration and mixing phases were stopped once the set durations were reached. In particular, in both SBRs the duration of the aeration phases was manually adjusted with the aim of not exceeding the value of 20 mg NO_x^--N·L^{-1}, as sum of concentration of nitrite and nitrate after the aeration. The duration of the mixing phases was set to achieve the full consumption of the NO_x^- produced during the previous aeration phase. The number of aeration and mixing phases was also manually adjusted in order to not exceed the concentration of 50 mg TAN·L^{-1} at the end of the cycle.

The aeration phase was conducted under oxygen limitation in the SBR_A ($0.8 < DO < 1.2$ mg L^{-1}) to both obtain PN and avoid AAO inhibition, while oxygen in the SBR_B was maintained at 2–3 mg O_2 L^{-1} to better support the nitrification process. A final mixing phase was expected in both SBRs to ensure the completion of denitrification. A time-controlled sedimentation phase, followed by a discharge phase, was finally provided, its duration being fixed based on sludge characteristics.

Table 1 reports the main operational parameters of the two SBRs and the details of the applied process cycles during the observed periods. The average temperature in the two SBRs was 23.3 ± 1.5 °C in Period I, 17.1 ± 1.5 °C in Period II, and 10.5 ± 2.0 °C in Period III.

Table 1. Operating characteristics of SBRs.

	Parameter	Period I	Period II	Period III
SBR_A	Average V_{fill} (m^3 d^{-1})	53.5 ± 13.3 (0–109.4)	57.9 ± 26.8 (0–117.8)	54.1 ± 26.7 (0–113.1)
	NLR (kg N m^{-3} d^{-1})	0.029 ± 0.008 (0–0.052)	0.037 ± 0.019 (0–0.064)	0.036 ± 0.017 (0–0.068)
	HRT (d)	16.3 ± 1.2	16.3 ± 7.4	17.2 ± 6.6
	n cycle per day	2	1–2	2
	TSS (g L^{-1})	1.6 ± 0.4	1.5 ± 0.1	2.0 ± 0.2
	VSS (g L^{-1})	1.3 ± 0.4	1.4 ± 0.1	1.7 ± 0.1
			Typical SBR cycle	
	SBR cycle (h)	(10)	(10)	(12)
	Leachate Fill (min)	(70)	(70–75)	(40–70)
	Buttermilk Fill (m^3/cycle)	0.036 ± 0.100 (0–0.30)	0	0.310 ± 0.150 (0–0.60)
	Initial Mixing (min)	(140)	(90–140)	(90–150)
	Aeration (min) • number of aeration	(20–22) • 3	(20–26) • 3	(20–26) • 6
	Buttermilk Fill	-	0.01 ± 0.03 (0–0.10)	0.01 ± 0.03 (0–0.10)
	Mixing (min) • number of mixing	(55–60) • 3	(50–60) • 3	(40–66) • 6
	Final mixing (min)	(100)	(100–140)	(20–140)
	Sedimentation (min)	(40)	(40)	(40)
	Draw (min)	(15)	(15)	(10)
SBR_B	Average V_{fill} (m^3 d^{-1})	46.8 ± 14.9 (0–87.4)	42.4 ± 21.8 (0–104.6)	38.2 ± 15.5 (0–73)
	NLR (kg N m^{-3} d^{-1})	0.025 ± 0.008 (0–0.042)	0.021 ± 0.011 (0–0.050)	0.027 ± 0.010 (0–0.047)
	HRT (d)	16.8 ± 8.0	19.8 ± 7.2	24.7 ± 9.3
	n cycle per day	2	2	2
	TSS (g L^{-1})	1.87 ± 0.1	1.01 ± 0.06	1.53 ± 0.1
	VSS (g L^{-1})	1.46 ± 0.1	0.98 ± 0.04	1.46 ± 0.04
			Typical SBR cycle	
	SBR cycle (h)	(10)	(10–12)	(10–12)
	Leachate Fill (min)	(60–70)	(30–65)	(30–60)
	Buttermilk Fill (m^3/cycle)	0	0	0
	Initial Mixing (min)	(140–150)	(140–150)	(100–230)
	Aeration (min) • number of aeration	(45–75) • 1	(30–130) • 1	(60–200) • 1
	Buttermilk Fill (m^3/cycle)	0.042 ± 0.050 (0–0.10)	0.084 ± 0.093 (0–0.3)	0.330 ± 0.136 (0.10–0.60)
	Mixing (min) • number of mixing	(150–230) • 1	(180–230) • 1	(200–250) • 1
	Final mixing (min)	(60–100)	(90–120)	(80–120)
	Sedimentation (min)	(40)	(40)	(40–100)
	Draw (min)	(15)	(15)	(10–15)

Data are expressed as mean ± s.d., and [min–max]; Vfill = Filled volume of leachate per day.

2.2. Data Collection

A long-term sampling campaign was carried out on the full-scale leachate treatment plant for a period of five months (29 August 2016–30 January 2017). The monitoring campaign has been split into three periods of about 1.5 months each. The first period (Period I) from 29 August to 20 October 2016, the second period (Period II) from 21 October to 9 December 2016, and the third period (Period III) from 10 December 2016 to 30 January 2017. The main differences among the three periods were in the external temperature, leachate characteristics and some changes made to the operational conditions of the treatment plant. During these periods, biweekly measurements of TAN in the influent and effluent of the leachate treatment plant and periodical TNN and NO_3^-N analyses were carried out.

Furthermore, three intensive sampling campaigns were conducted at the end of each monitoring period, i.e., track studies. During the track studies, SBR samples were collected at the beginning and end of each phase of the cycle to evaluate the concentrations of TAN, total nitrite nitrogen (TNN), NO_3^--N, and soluble chemical oxygen demand (sCOD). Mixed liquor samples were also collected for total suspended solids (TSS) and volatile suspended solids (VSS) analyses.

2.3. Landfill Leachate Characteristics

The chemical composition of the influent raw leachate treated during the different simulation periods is summarized in Table 2. It can be observed that in Periods I and II the leachate was characterized by a low biochemical oxygen demand (BOD_5)/COD (<0.1), indicating a scarce biodegradability level (as typical of mature leachate [22]). On the contrary, in Period III the leachate was characterized by a higher biodegradability (BOD_5/COD = 0.40) due to the opening of a new area in one of the landfills.

Table 2. Characteristics of the influent raw leachate in each experimental period.

Parameter	Period I	Period II	Period III
BOD_5 (mg L^{-1})	57 ± 4 (54–60)	47	330
sCOD (mg L^{-1})	693 ± 227 (431–838)	557 ± 113 (431–649)	814 ± 234 (649–980)
TAN (mg L^{-1})	507 ± 132 (406–656)	466 ± 61.3 (408–530)	608 ± 111 (530–686)
NO_x-N (mg L^{-1})	6.1 ± 0.4 (5.5–7.1)	6.0 ± 0.6 (5.2–7.1)	5.4 ± 0.1 (5.1–5.6)
BOD_5/COD	0.07	0.08	0.40
COD/TAN	0.94- 2.1	0.94–1.45	1.22–1.43
TP (mg L^{-1})	5.1 ± 0.9 (4.3–7.2)	5.2 ± 1.1 (3.5–7.2)	8.8 ± 1.4 (6.4–11.2)
pH	(7.8–8.2)	(8.1–8.2)	(8.1–8.2)
Alkalinity as $CaCO_3$ (mg L^{-1})	2000	2000	2000

Data are expressed as mean ± s.d. and [min–max].

2.4. Buttermilk Characteristics

The buttermilk used as a supplemental source of organic carbon for the two SBRs was a by-product of a nearby dairy butter industry. The average values of the parameters during the whole monitoring campaign were: 52 g total COD (tCOD) L^{-1}, 43 g sCOD L^{-1}, 980 mg total Kjeldahl nitrogen (TKN) L^{-1}, 280 mg TAN L^{-1}, 0.04 mg TNN L^{-1}, 140 mg NO_3^--N L^{-1}, 470 mg total phosphorus (TP) L^{-1}, 50 mg PO_4-P L^{-1}, 1460 mg $CaCO_3$, 0.99 mg TSS L^{-1}, 0.90 mg VSS L^{-1}.

2.5. Model Set-Up

2.5.1. Modelling—Biokinetic Model

The biological nitrogen removal was simulated by using the BioWin software version 6.0 (EnviroSim Associates Ltd., Canada) [23], based on the Activated Sludge/Anaerobic Digestion model (ASDM). The BioWin ASDM is composed of 174 processes acting on 83 state variables, able to describe the typical chemical and biological processes occurring in a WWTP [24]. The overall model includes: activated sludge process, anaerobic digestion processes, sulfur conversion processes, chemical precipitation reactions, pH and alkalinity variation, modelling of industrial components and general parameters. In this work, the most relevant biological processes are those related to carbon and nitrogen degradation: growth and decay of OHO, growth and decay of AOB, growth and decay of NOB, growth and decay of AAO. Therefore, only the kinetic and stoichiometric parameters related to these processes have been used in the calibration under aerobic and anoxic conditions.

2.5.2. Modelling—Plant Configuration

Figure 1 shows a simplified flow scheme of one single treatment line of the leachate treatment plant as built in the BioWin environment. The influent leachate ("COD influent" element) and the external carbon source, i.e., buttermilk, ("state variable influent" element) were separately represented. Each SBR was modelled using a "single-tank SBR" bioreactor element (without pre-zones) where filling, settling and decanting phases occur in one zone without baffles. Finally, the model configuration comprises the "effluent" and the" sludge" elements. In the full-scale SBR_A plant configuration, unlike the DEMON process, the hydrocyclone has not been used to recover the anammox biomass from the waste sludge stream, but only to separate flocs and granules, without any biomass wastage. All fluxes from the hydrocyclone are recycled back to the SBR. In the BioWin model, in both SBRs, the

"separator-cyclone" element has been employed to increase the sedimentation efficiency of the anammox biomass and it has been inserted in the effluent line as a stratagem, taking into account the higher settleability of the micro-granular biomass.

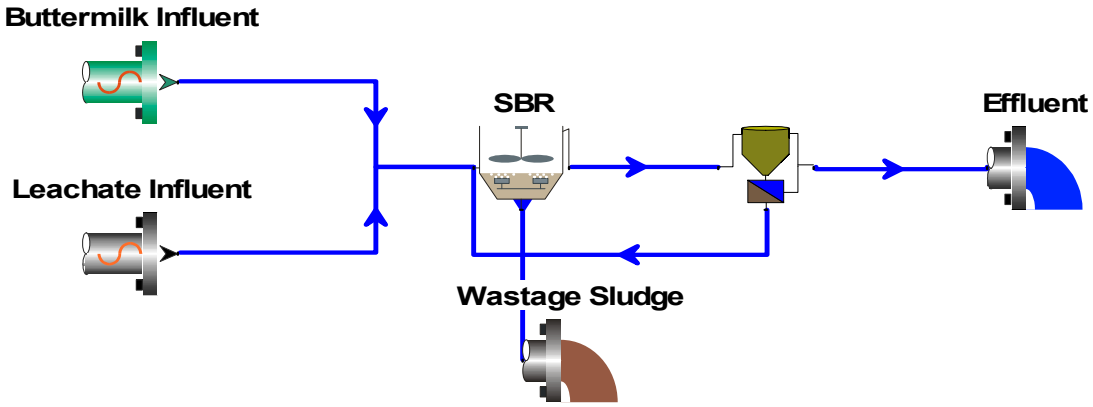

Figure 1. Schematic flow diagram for the leachate treatment plant as implemented in BioWin.

The sludge effluent was set to 0 m^3 d^{-1} for both SBRs because no sludge extraction was carried out during the entire monitoring campaign. In the calculation of SRT, the TSS washed out with the effluent have been considered.

SBR dimensions (i.e., volume, depth and minimum decant level), operational conditions (i.e., cycle length, filling, reaction, settling and decanting periods, local temperature), initial settings for the SBR element, concentrations and volume, power specifications for mechanical mixing, SBR overflow behaviour and model options (such as settling phase behaviour, kinetic parameters, aeration and diffuser model settlings, etc) were employed in accordance with the full scale application.

The BioWin Controller was employed to simulate the aeration process in the SBRs, consisting in an on/off control based on oxygen monitoring. In SBR_A, the air supply started at 0.8 mg O_2 L^{-1} and stopped at 1.2 mg O_2 L^{-1} while in SBR_B it started at 2.0 mg O_2 L^{-1} and stopped at 3.0 mg O_2 L^{-1}.

The input parameter values of the flow rate, nitrogen inflow concentrations (TAN, TNN, NO_3^--N), COD, phosphorous, alkalinity and pH of both leachate and buttermilk were set in each conducted simulation in accordance with monitoring data.

Leachate fractions of tCOD, TKN, TP and sulphur (S), used in the BioWin model in the different simulation periods are reported in Table 3. The degradability of the organic matter was assessed by fractionation experiments. The numerical values not analytically measured were estimated based on literature monitoring and experimental studies on leachate composition. In order to account for the much higher soluble fraction of the organic matter in the landfill leachate in Period III as compared to Period I and II (Table 2), readily biodegradable COD (Fbs) was increased, while unbiodegradable soluble COD (Fus) was decreased.

The initial biomass values were calculated through the repeated execution of a typical cycle of the two SBRs until obtaining the convergence on stable values of the concentrations of the different types of biomass present in the reactor.

Table 3. Leachate fractions used in BioWin models.

Components	Unit	Period I	Period II	Period III
Fbs—readily biodegradable organic matter (including acetate) *	g COD g tCOD $^{-1}$	0.0150	0.0150	0.1500
Fac- acetate *	g COD g rbCOD^{-1}	0.0001	0.0001	0.0001
Fxsp—Non colloidal slowly degradable	g COD g sdCOD^{-1}	0.7500	0.7500	0.7500
Fus—Unbiodegradable soluble COD *	g COD g tCOD^{-1}	0.8240	0.8240	0.6890
Fup—unbiodegradable particulate COD *	g COD g tCOD^{-1}	0.003	0.003	0.003
Fcel—Cellulose fraction of unbiodegradable particulate	g COD g tCOD^{-1}	0.5000	0.5000	0.5000
Fna—Ammonia *	g NH_4-N gTKN^{-1}	0.9400	0.9400	0.9400
Fnox—Particulate organic nitrogen	g N g Organic N^{-1}	0.5000	0.5000	0.5000
Fnus—Soluble unbiodegradable TKN	g N gTKN^{-1}	0.0200	0.0200	0.0200
FupN N:COD ratio for unbiodegradable part. COD	g N g tCOD^{-1}	0.0700	0.0700	0.0700
Fpo4—Phosphate	g PO_4-P gTP^{-1}	0.5000	0.5000	0.5000
FupP—P:COD ratio for unbiodegradable part. COD	g P g tCOD^{-1}	0.0220	0.0220	0.0220
Fsr—Reduced sulfur [H_2S]	g S g S^{-1}	0.1500	0.1500	0.1500
FZbh—Ordinary heterotrophic COD fraction	g COD g tCOD^{-1}	0.0200	0.0200	0.0200
FZbm—Methylotrophic COD fraction	g COD g t COD^{-1}	0.0001	0.0001	0.0001
FZao—Ammonia oxidizing COD fraction *	g COD g tCOD^{-1}	0.001	0.001	0.001
FZno—Nitrite oxidizing COD fraction *	g COD g tCOD^{-1}	0.001	0.001	0.001
FZaao—Anaerobic ammonia oxidizing COD fraction	g COD g tCOD^{-1}	0.0001	0.0001	0.0001
FZppa—Phosphorus accumulating COD fraction	g COD g tCOD^{-1}	0.0001	0.0001	0.0001
FZpa—Propionic acetogenic COD fraction	g COD g tCOD^{-1}	0.0001	0.0001	0.0001
FZam—Acetoclastic methanogenic COD fraction	g COD g tCOD^{-1}	0.0001	0.0001	0.0001
FZhm—Hydrogenotrophic methanogenic COD fraction	g COD g tCOD^{-1}	0.0001	0.0001	0.0001
FZso—Sulfur oxiding COD fraction	g COD g tCOD^{-1}	0.0001	0.0001	0.0001
FZsrpa—Sulfur reducing propionic acetogenic COD fraction	g COD g tCOD^{-1}	0.0001	0.0001	0.0001
FZsra—Sulfur reducing acetotrophic COD fraction	g COD g tCOD^{-1}	0.0001	0.0001	0.0001
FZsrh—Sulfur reducing hydrogenotrophic COD fraction	g COD g tCOD^{-1}	0.0001	0.0001	0.0001
FZe—Endogenous products COD fraction	g COD g tCOD^{-1}	0	0	0

* Modified from BioWin default values; rbCOD = readily biodegradable COD; sdCOD = slowly degradable COD.

2.5.3. Model Calibration and Validation

The iterative procedure applied to calibrate and validate the model is based on 6 steps, as proposed by Rieger [25] (Supplementary Material, Figure S3): (1) identification of different simulation periods for both calibration and validation processes; (2) initial model run based on BioWin defaults kinetics and stoichiometric parameters values, in order to define a first output and draw a comparison with measured data; (3) selection of the most sensitive parameters for the model calibration process and definition of their acceptable range of variation, based on expert knowledge and literature data; (4) calibration of the model until the admissible error limits are respected, for the selected data period; (5) validation of the model through the comparison between simulation results and observed data on a different data period; (6) discussion with the stakeholders (i.e., leachate treatment plant owner and manager) and their approval.

Model calibration was carried out using the monitoring data collected during Periods I and II (Table 4). The validation step was then carried out with the calibrated model by

using the monitoring data collected during Period III, characterized by different inflow conditions and SBR operational conditions (Table 4).

Table 4. Monitoring periods for model calibration and validation.

Process	Reactor	Periods	Date
Calibration	SBR_A	Period I	29 August 2016–19 October 2016
		Track study I	20 October 2016
		Period II	21 October 2016–6 December 2016
		Track study II	7 December 2016
	SBR_B	Period I	29 August 2016–19 October 2016
		Track study II	20 October 2016
		Period II	21 October 2016–8 December 2016
		Track study II	9 December 2016
Validation	SBR_A	Period III	8 December 2016–25 January 2017
		Track study III	26 January 2017
	SBR_B	Period III	10 December 2016–29 January 2017
		Track study III	30 January 2017

2.5.4. Chemical Analyses and Physical Data

During the long-term monitoring campaign, samples of influents and effluents collected from the two SBRs were filtered through Whatman GF/F filters (0.45 micron). The filtrate was analyzed spectrophotometrically for TAN, TNN and NO_3^--N concentrations according to the Standard Methods [26]. The organic matter content of the wastewater expressed as tCOD, sCOD and BOD_5 as well as TSS, VSS, TP and S concentrations in the mixed liquor and effluent were further determined according to the Standard Methods [26]. Other variables such as influent flow rate, aerator operational data (aerator working frequency), online DO and pH data were obtained from plant operators.

3. Results and Discussion

The developed model successfully simulated the nitrogen removal processes occurring in the two real SBR treatment systems. The model contributed to better understand the role of the biomass involved in the processes. In the following sections, the nitrogen removal efficiencies together with calibration and validation results are presented and discussed. Further, results on biomass contribution to nitrogen removal and nitrous oxide (N_2O) emission are presented.

3.1. Nitrogen Removal Performance

The SBR performances in terms of nitrogen removal slightly varied during the monitoring periods, mainly due to temperature decrease moving from Period I to Period III. Overall, both SBRs achieved high nitrogen removal efficiencies.

SBR_A was characterized by higher NLRs and a lower variability of TAN removal efficiencies compared to SBR_B. However, TAN removal efficiencies over 88% were achieved in both SBRs.

In SBR_A, operated with NLRs of 26 ± 7 (Period I), 34 ± 17.5 (Period II), and 33 ± 16 kg N d^{-1}(Period III) (Table 1), TAN removal efficiencies were in the range of 93.1–99.0% (96.0 ± 1.4%) in Period I, 90.4–97.3% (93.8% ± 1.7%) in Period II, and 88.2–95.5% (92.1% ± 2.5%) in Period III. The corresponding average TAN concentrations in the effluent were 19 ± 6, 28 ± 7, and 47 ± 15 mg TAN L^{-1}, while the effluent TNN concentrations were 0.14 ± 0.07, 0.98 ± 0.65, and 2.9 ± 1.77 mg TNN L^{-1}, respectively in Period I, II and III. Nitrate effluent concentrations were always lower than 5.0 mg NO_3^--N L^{-1}. Moving from Period I to Period III, in order

to compensate for the lower kinetics of AOB at lower temperatures, the cycle duration was increased from 10 to 12 h and aeration phases were prolonged. An increasing fraction of buttermilk was added during the first mixing phase when nitrite concentration in the effluent of the previous cycle was higher than 2.0 mg TNN L^{-1}, mainly in Period III, in order to reduce nitrite accumulation in the SBR by means of denitrification, thus preventing anammox inhibition in the PN/A process [21].

The SBR_B was operated with a 13%, 45% and 25% lower NLR compared to SBR_A in Period I, II and III, respectively. TAN removal efficiencies were in the range of 89.7–99.0% (95.7% ± 2.6%), 89.4–97.9% (93.6% ± 2.6%), and 90.2–98.0% (93.6% ± 2.3%) in Period I, II and III, respectively. The corresponding average TAN concentrations measured in the effluent were 21 ± 11 (Period I), 28 ± 11 (Period II), and 41 ± 15 (Period III) mg NH_4^+-N L^{-1}, while the effluent nitrite concentrations were 0.3 ± 0.2 (Period I), 2.8 ± 4.8 (Period II), and 4.5 ± 8.2 (Period III) mg TNN L^{-1}. Similarly to SBR_A, nitrate effluent concentrations were always lower than 5.0 mg NO_3^--N L^{-1}. Again, moving from Period I to Period III the cycle duration was increased from 10 to 12 h and aeration phases were prolonged to compensate for the lower kinetics of AOB at lower temperatures. In SBR_B, buttermilk was dosed immediately after the aeration phases and was gradually increased from Period I to Period III to favor denitrification in the SPND process, thus optimizing nitrogen removal.

As described in the following section, the model simulations showed that both SBRs were based on anammox processes, where NOB were inhibited and with different contributions of denitrification to nitrogen removal. Nhat et al. [27] reported similar TAN removal performance by a two stage PN/A system for the treatment of old landfill leachate, but under higher NLRs (4.2–8.3 kg N m^{-3} d^{-1}) compared to those applied in this study (0–0.069 kg N m^{-3} d^{-1}). The reason for this might be the much higher biomass content in the two reactors, that allowed to increase the loading rates. Indeed, in their one-stage SBR treating leachate by means of simultaneous PN, anammox and denitrification, Wang et al. [28] obtained lower TAN removal efficiencies under NLRs of 0.118–0.280 kg N m^{-3} d^{-1}.

3.2. Model Calibration

The model calibration targeted the estimation of the best-fit parameters for a specific given set of real data acquired from the monitored leachate treatment plant. Data for Periods I and II were used for calibration. The simulations were started with the default values of the model which were later adjusted to match the observed results collected from the full-scale SBRs. Table 5 compares the kinetic parameters used for model calibration of both SBR_A and SBR_B performances to their default values in BioWin [24] and literature data. The parameters used for model calibration have been selected based on local sensitivity evaluations. Several runs were performed adjusting the selected kinetic and stoichiometric parameters (Table S1) to obtain the best matching between model output and the plant effluent quality data.

Table 5. Parameter values adjusted during model calibration.

Parameters	Unit	SBR_A	SBR_B	BioWin Default	Literature Range	Reference
Max. spec. growth rate, $_{AOB}$	d^{-1}	1.0	1.0	0.9	0.33–1.02	[29]
Substrate (NH_4) half sat, $_{AOB}$	mg N L^{-1}	26.6	26.6	0.7	12.2–46.2	[30–32]
Aerobic decay rate, $_{AOB}$	d^{-1}	0.035	0.035	0.17	0.02–0.17	[29,33–35]
Anoxic decay rate, $_{AOB}$	d^{-1}	0.035	0.035	0.08	0.02–0.11	[29,33,34]
Aerobic decay rate, $_{NOB}$	d^{-1}	0.07	0.07	0.17	0.07–0.17	[35–38]
Anoxic/anaerobic decay rate, $_{NOB}$	d^{-1}	0.07	0.07	0.08	0.07–0.15	[36,37]
Aerobic decay rate, $_{AAO}$	d^{-1}	0.0095	0.0095	0.019	0.0048–0.016	[39–42]
DO half sat, $_{AOB}$	mg O_2 L^{-1}	0.125	0.25	0.25	0.04–0.48	[43]
DO half sat, $_{NOB}$	mg O_2 L^{-1}	0.25	0.50	0.50	0.17–4.33	[32]

The calibrated parameters were the same for both SBRs, except for the DO half saturation constant of AOB and NOB. The lower values used for SBR_A compared to SBR_B can be justified by the significantly lower oxygen concentrations in SBR_A compared to SBR_B, as such conditions may promote the selection of more efficient bacteria at lower DO levels [32,43]. AOB maximum specific growth rate (1.0 d^{-1}) was slightly increased compared to the BioWin default value (0.9 d^{-1}). Contrary to mainstream nitrogen removal systems, there are only a few studies about determination of the decay rate of nitrifiers and anammox bacteria in side-stream systems treating high-strength ammonium-contaminated wastewater (i.e., landfill leachate). In this study, the aerobic and anoxic decay rates of AOB, NOB and AAO were decreased as compared to BioWin default values as a result of model calibration. However, the values fell within the literature ranges. Concerning AOB, Munz et al. [34] showed that the decay rate is very sensitive to DO concentration, reaching values as low as 0.031 d^{-1} under anaerobic conditions. Low aerobic decay rates for NOB have been fixed in accordance with previous research that reported values of 0.04 d^{-1} for NOB biomass, where, like in this study (data to be published), *Nitrospira* spp. was the dominant genus [38]. The similar decay rates of AOB and NOB found in this research are in agreement with the findings by other researchers [33,36,38]. Finally, the decay rate of AAO was justified by microbial analysis that showed the presence in both SBRs of *Candidatus Scalindua* (data to be published), which is characterized by decay rates (0.006 d^{-1}) lower than BioWin default values (0.019 d^{-1}) [41].

The ammonia half saturation constant of AOB was significantly increased from 0.7 to 26.6 mg N L^{-1} in accordance with the fact that the high ammonia levels in both SBRs allowed for selecting a biomass with low affinity for the substrate [44]. This was further confirmed by a specific microbiological characterisation of nitrifying bacteria that identified *Nitrosomonas* spp., which are characterized by high values of the ammonia half saturation constant, as the main AOB genera in both reactors (data to be published).

Figure 2 shows the track studies simulated by the calibrated model for SBR_A (Figure 2a,c) and SBR_B (Figure 2b,d). The comparison between the measured and simulated effluent nitrogen concentrations showed a similar trend and was considered satisfactory for both SBRs. The models also successfully reproduced the sCOD values at the end of each cycle for both SBRs. The average percentage difference between simulated and measured data in sCOD was −4% and +11% in SBR_A and SBR_B, respectively (Table S2). When performing long-term term simulations in Period I and II between the track studies, the models acceptably reproduced the effluent nitrogen concentrations (Figure S4).

3.3. Model Validation

After calibration, the model was validated using experimental data from Period III. All stoichiometric and kinetic parameters were set to the values identified within the calibration step. The influent stoichiometric fractions (Table 3) and the influent leachate quality were set to the average values of the third experimental period (Table 2). The results of the model validation confirmed a good data reproduction for both reactors. Figure 3 shows the track studies simulated by the validated model for SBR_A (Figure 3a) and for SBR_B (Figure 3b). Effluent nitrogen concentrations measured during the long-term sampling campaign in Period III could be satisfactorily reproduced by models (Figure S4).

The calibrated models performed well in describing the biological processes at the leachate treatment plant both in SBR_A and SBR_B.

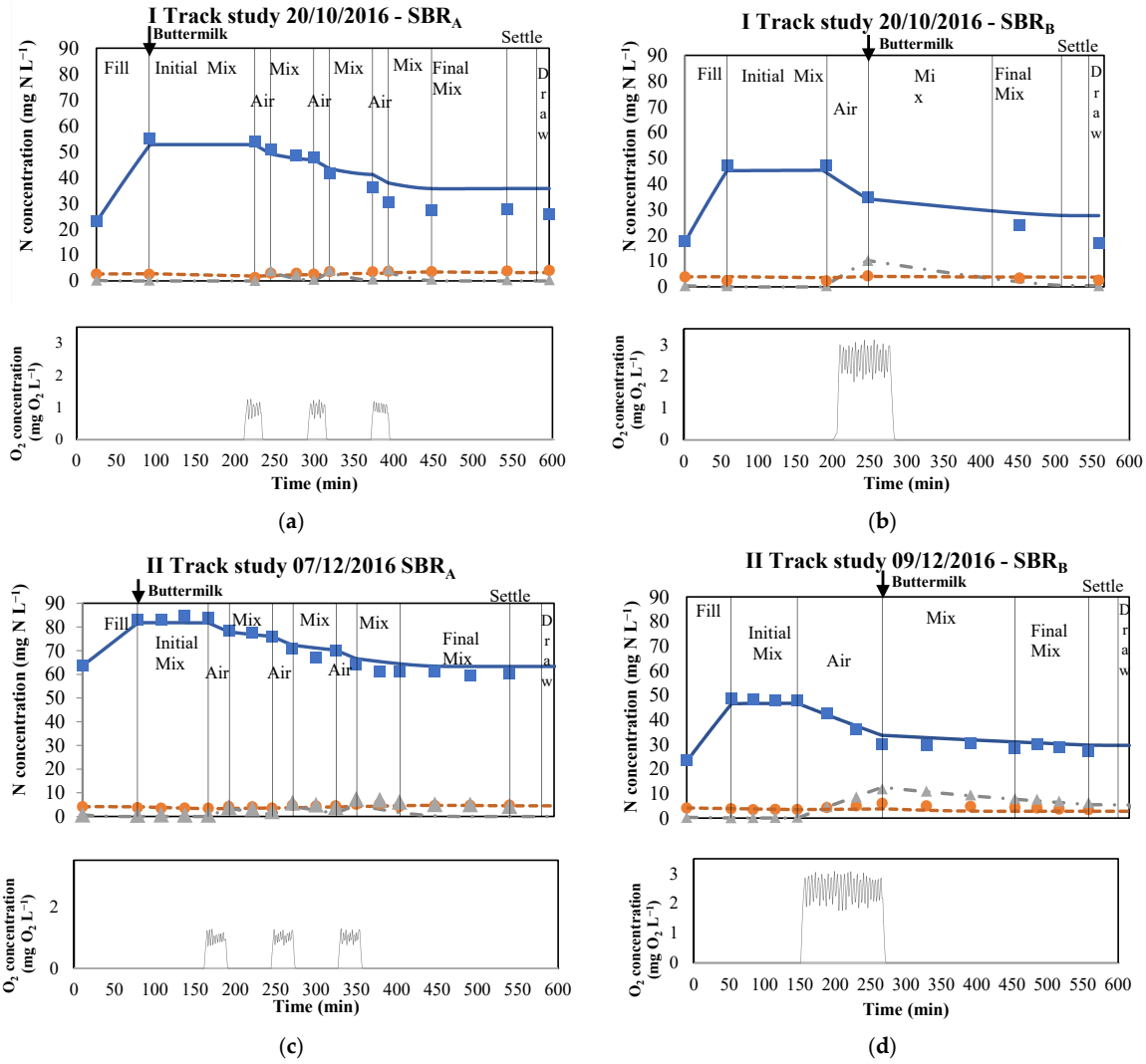

Figure 2. Comparison of measured (TAN, TNN, NO_3^--N) and simulated (TAN, TNN, NO_3^--N) and simulated (TAN, TNN, NO_3^--N) nitrogen effluent concentrations during the track studies for SBR$_A$ (**a**,**c**) and SBR$_B$ (**b**,**d**) calibration. DO values.

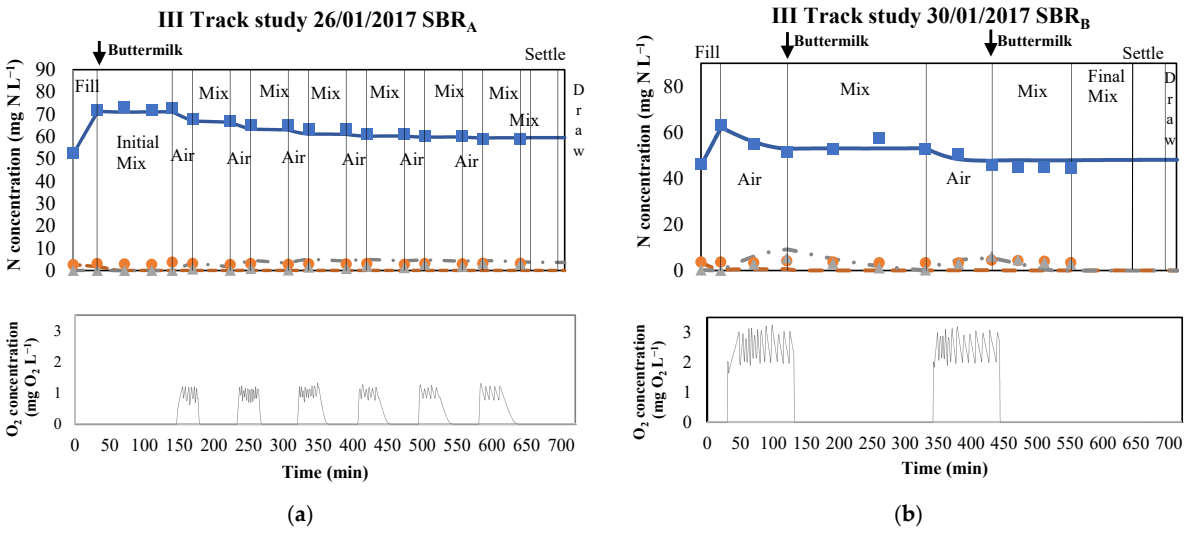

Figure 3. Comparison of measured (TAN, TNN, NO_3^--N) and simulated (TAN, TNN, NO_3^--N) effluent nitrogen concentrations during the track studies for SBR$_A$ (**a**) and SBR$_B$ (**b**) validation. DO values.

3.4. SBR Cycle Analysis

Figures 2 and 3 show the profiles of nitrogen species during the track studies performed with both SBRs, distinguishing the aerobic and the mixing phases. From the analysis on the graphs an almost similar pattern can be identified for all investigated track studies.

At first, during the leachate feeding phase, TAN concentration increased in both SBRs reaching maximum values in the range of 50–85 mg TAN L^{-1}, corresponding to FA concentrations ranging from 0.48 to 1.74 mg NH_3-N L^{-1} [45] depending on the Period (Table 6), which could negatively affect NOB activity. Indeed, Kim et al. [46] reported that NOB related to *Nitrospira* spp. were inhibited at 0.04–0.08 mg NH_3-N L^{-1}.

Table 6. Peak of NH_3 concentration in each SBR cycle and I_{NH3} values in SBR_A and in SBR_B.

	SBR_A				**SBR_B**			
	Peak of NH_3 concentration in each SBR cycle [mg N L^{-1}]							
	Min	Avg	Max	pH range	Min	Avg	Max	pH range
Period I	0.044	0.572	1.74	7.3–7.9	0.038	0.525	1.70	7.4–7.9
Period II	0.043	0.387	1.21	7.3–7.5	0.057	0.539	1.22	7.3–7.5
Period III	0.001	0.069	0.480	4.7–7.2	0.001	0.139	0.479	5.0–7.4
	Peak I_{NH3} value in each SBR cycle *							
	Min	Avg	Max		Min	Avg	Max	
Period I	0.96	0.65	0.38		0.97	0.67	0.38	
Period II	0.96	0.73	0.46		0.95	0.66	0.46	
Period III	1.00	0.94	0.69		1.00	0.88	0.69	

Min = minimum, Avg = Average; Max = maximum; * Where 1.0 means no inhibition.

This phase was followed in the SBR_A by the addition of an external carbon source and by an anoxic mixing phase of variable duration, that allowed a slight reduction of the residual nitrate and nitrite from the previous cycles. In the SBR_B, the leachate filling phase was directly followed by an anoxic mixing phase or an aerobic phase.

Then, a proper reaction phase started in both SBRs. The SBR_A was characterized by short aerobic and anoxic repeated phases to promote the PN/A process, while in the SBR_B one longer aerobic phase was carried out, followed by one longer anoxic phase to promote the SPND process. In both SBRs, during the aerobic phases, a decrease of TAN concentration, with a resulting TNN concentration increase due to AOB activity, could be observed. NOB were inhibited in SBR_A due to the high FA concentrations reached at the beginning of the SBR cycles (Table 6) and to the low DO concentrations [45], thus nitrate concentrations did not increase during the aerobic phases. In SBR_B, where FA concentrations were also high but DO concentration was not inhibitory, nitrate concentration slightly increased due to a low NOB activity.

Nevertheless, the model showed that peaks of FA in SBR cycle decreased from Period I to Period III. This was attributed to the decreasing temperatures and lower pH values (<6.5) in both SBRs (Table 6) as a consequence of the addition of younger leachate characterized by a lower alkalinity/ammonia ratio, being insufficient for nitrification. The inhibition factor (I_{NH3}) for NOB, calculated as $Ki_{NH3}/(Ki_{NH3} + NH_3)$ with Ki_{NH3} (inhibition constant) equal to 1.05 mg N L^{-1}, was in the range of 0.65–0.73, meaning that NOB activity was inhibited by about 27–35% in both SBRs. In Period III, the I_{NH3} increased in both SBRs (Table 6), meaning that the inhibition of NOB by FA was lower, but pH values below 6.5 likely caused the complete inhibition of the NOB activity [47], half-inhibiting the AOB activity [48].

During the anoxic phase in SBR_A, a simultaneous decrease of TAN and TNN concentrations was observed in all tested periods at temperatures of 23.3 ± 1.5 °C, 17.1 ± 1.5 °C and 10.5 ± 2.0 °C, respectively, which was referred to the anammox activity. Nitrate profile did not increase during the anoxic phases, meaning that denitrification was coupled with the anammox process.

In the SBR_B, the anoxic mixing phases were preceded by the addition of an external carbon source to promote denitrification. However, when temperature higher than 17.1 ± 1.5 °C (Periods I and II) occurred, the required carbon dosage was minimum and a decrease of TAN concentration during the anoxic phase was also observed in the SBR_B, meaning that the anammox process was also active, despite the DO values of 2–3 mg O_2 L^{-1} in the aerobic phases. Anammox bacteria, as obligate anaerobes, are inhibited by exposure to DO, with 50% inhibitory concentrations ranging from 0.03 to 3.8 mg O_2 L^{-1} [49]. This variability in the reported DO inhibitory levels can be due to inter-genera differences [50], potential adaptation towards oxygen stress, and protection by oxygen consuming bacteria in small aggregates [51]. In particular, *Scalindua* species, as those detected in this study, were shown to withstand the increase of oxygen concentration in the system [52]. Furthermore, various observations from engineering applications have shown that anammox bacteria can "reversibly" recover from DO inhibition [53]. Lotti et al. [54] showed that the presence of oxygen (up to 5 mg L^{-1}) completely inhibited the conversion of ammonium and nitrite during the exposure phase, but anammox biomass was still active in the following anoxic phase, with an activity reduction of less than 10% compared to bacteria not exposed to oxygen. Recent studies showed that recovery of anammox after oxygen exposure was previously overlooked and it is recommended to account for this effect in the intensification of PN/A [49].

During Period III, as a precaution for the low temperature (10.5 ± 2.0 °C), aeration phases were prolonged in both SBRs (Figure 3), and a higher carbon dosage was provided to the plant. The external carbon dosage was higher in SBR_B. Thus, as could be seen by the TAN profile during the anoxic phase, the anammox activity was significantly reduced due to the competition between anammox and denitrifying bacteria (Figure 3b).

Finally, at the end of the cycle, in both SBRs, a mixing phase was carried out, but no significant variation in concentration of the monitored parameters was observed.

3.5. Biomass Concentration Trend

Biomass concentration trends for all the experimental periods in both SBRs are shown in Figure 4.

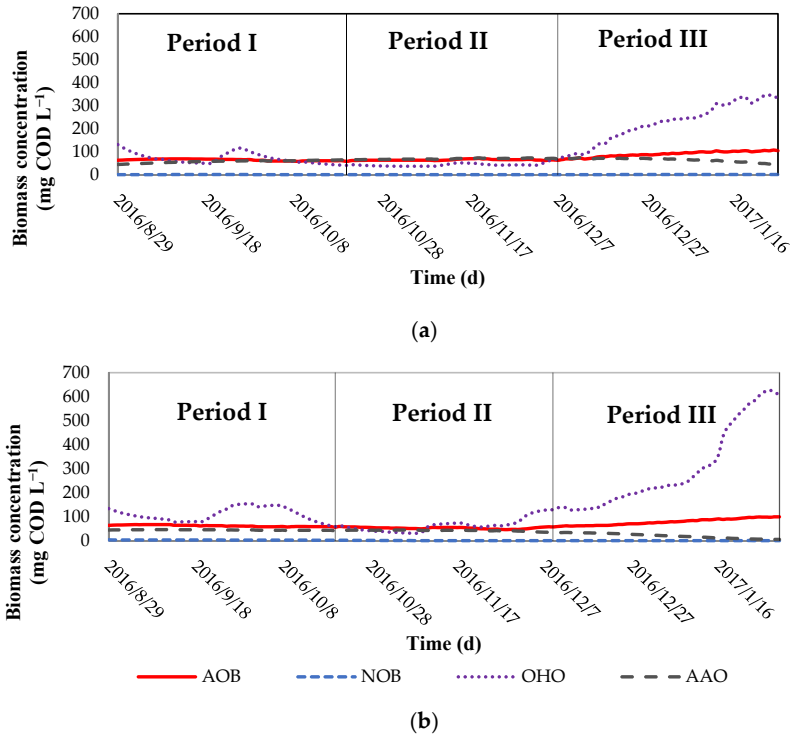

Figure 4. Simulated biomass trend in SBR_A (**a**) and SBR_B (**b**).

The fluctuations of OHO biomass correspond very well to the variation of external carbon source (i.e., buttermilk) dosage in the reactors (Table 1). In both reactors, buttermilk addition was significantly incremented in winter months (Period III) with the aim of compensating with heterotrophic denitrification any anammox activity decrease caused by the lower temperatures. The presence of organic matter, either high COD concentrations or high COD/N ratio, is reported to affect the PN/A process adversely [55,56]. The buttermilk dosage was higher for SBR_B and, correspondingly, a higher increase of the heterotrophic biomass was observed in this reactor.

In both SBRs, the AOB biomass trends are quite constant, with a gradual slight growth in Period III caused by a slight increase of nitrogen load, despite a partial inhibition of AOB by pH values lower than 6.5 as a consequence of younger leachate addition. Growth inhibition of NOB was induced in SBR_A by setting a low DO concentration in the aeration phases [57], but due to the high concentrations of FA at the beginning of each reaction phase in SBR cycle (Table 6) it was successfully obtained also in SBR_B [45,58]. As reported in Section 3.4, during Period III, the complete inhibition and washout of NOB was likely achieved in both SBRs by pH values lower than 6.5.

AAO concentrations were significant in both reactors, as also detected by microbial analysis, which showed, similarly to Azari et al. [59], the presence of *Candidatus Scalindua* in both SBRs (data to be published). At the end of Period III, AAO concentrations had a decrease, almost complete in SBR_B but also notable in SBR_A, due to the competition with OHO bacteria for nitrite [60]. It is evident that the higher organic matter concentration negatively affected the growth of anammox bacteria. Therefore, an increase in the influent COD/N ratio becomes a concern when conducting anammox-based processes.

3.6. Contribution to Nitrogen Removal of AAO and OHO Biomass

Model simulations allowed to calculate the total contribution to nitrogen removal (measured as N_2 production) by both AAO and OHO biomass (Table 7). As expected, in SBR_A there was a significant activity of AAO biomass and the N_2 production by means of anammox bacteria was always predominant compared to that of OHO. Nevertheless, AAO biomass contribution in SBR_B, where the DO was set at 2–3 mg O_2 L^{-1}, was higher than that expected, due to the fact that anammox bacteria are characterized by a high variability of 50% inhibitory concentrations and further, they can reversibly recover from DO inhibition.

Table 7. Nitrogen removal predicted as N_2 production in SBR_A and in SBR_B.

	SBR_A			**SBR_B**	
	N_2 Production by AAO Bacteria (kg)	**N_2 Production by OHO Bacteria (kg)**		**N_2 Production by AAO Bacteria (kg)**	**N_2 Production by OHO Bacteria (kg)**
Period I (52 days)	1238	185	Period I (52 days)	991	282
Period II (47 days)	1044	109	Period II (49 days)	815	165
Period III (49 days)	1186	435	Period III (51 days)	489	663

During winter period (Period III), in correspondence with the increased buttermilk dosage and the discussed decrease of AAO biomass (Section 3.5), N_2 production related to AAO activity decreased in both SBRs, although it remained the main contributor to nitrogen removal in SBR_A. On the contrary, in SBR_B the contribution of denitrification with respect to the anammox process was higher. This suggests that SPND could occur in SBR_B during Period III.

Furthermore, by the employing of the model, the exact contribution to nitrogen removal (evaluated in terms of N_2 production, g N_2 $m^3_{reactor}$) of the AAO biomass during the

track studies was reproduced for both reactors and is shown in Figure 5. The contribution of AAO bacteria was significant in both SBRs, with a peak at the beginning of the anoxic phases. In the first track study (Figure 5a), a significant growth of AAO activity was observed during the anoxic phases following each aerobic phase, when both TAN and TNN are available for their metabolism. In both SBRs the AAO activity was very high despite the different aeration patterns (three shorter aeration phases for SBR_A, a single longer one for SBR_B), showing that both patterns are compatible with the PN/A process. Moreover, during the aerobic phase in the SBR_A a low AAO activity can be detected due to the low oxygen concentrations.

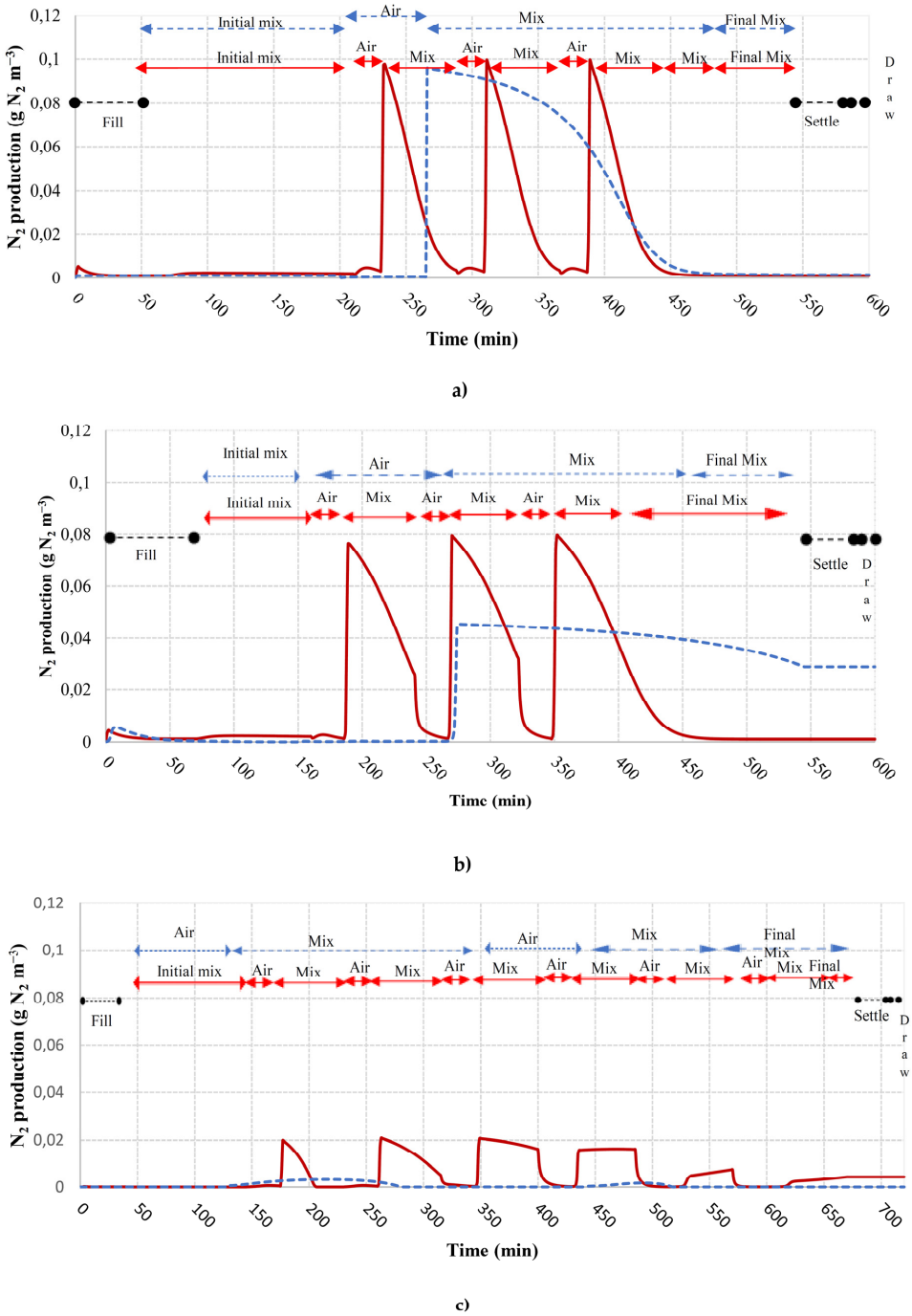

Figure 5. N_2 production (g N_2 $m^{-3}_{reactor}$) by AAO biomass in SBR_A (——) and in SBR_B (- - -) in the I (**a**), II (**b**) and III (**c**) track study. (◄►) Duration of aeration and mixing phases in SBR_A, (◄►) Duration of aeration and mixing phases in SBR_B, (●—●) Duration of filling, settle and draw phases in both SBRs.

In the second track study (Figure 5b), while the AAO activity in SBR_A only slightly decreased compared to the first track study due to lower temperatures, the AAO activity in SBR_B was halved also due to the higher dosage of buttermilk as compared to the first track study, that implied an increasing competition between AAO and OHO for NO_2^-. The last track study (Figure 5c), carried out at the end of the study, shows a much lower AAO activity in SBR_A compared to previous periods, mainly due to both lower temperatures and OHO competition with AAO. An almost inexistent AAO activity was detected in SBR_B in Period III due to both climatic conditions and strong competition with OHO bacteria for nitrite, as discussed above.

3.7. N_2O Production

During nitrogen transformations in biological processes, some of the removed nitrogen is emitted to the atmosphere as N_2O, which is an anthropogenic greenhouse gas (GHG). As the anammox process does not emit N_2O [61], in the studied SBRs N_2O can be produced by both OHO and AOB biomasses [62]. Heterotrophic N_2O production occurs when N_2O reductase is inhibited [63–66] by high TNN concentrations in the bulk liquid [67,68], or by organic carbon limitations [69]. AOB biomass can produce N_2O performing autotrophic denitrification under oxygen-limited conditions, high nitrite and low ammonia concentrations [70,71]. Furthermore, N_2O can be produced by AOB via hydroxylamine oxidation at high ammonia and low nitrite concentrations, and in combination with a high metabolic activity of AOB at 2–3 mg O_2 L^{-1} [69]. Emissions of N_2O from the PN/A and SPND processes are of concern and their evaluation is important to determine the carbon footprint of the processes. Recently, some studies showed that in PN/A approximately 70–80% of N_2O was produced during aerated phases by AOB, while the remaining 20–30% was produced during non-aerated phases by OHO [72,73]. N_2O emission from SPND of real mainstream wastewater in an intermittently aerated SBR accounted for 5.2% of removed TN and was mainly linked to build up of NO_2^- in the system at the end of the aerated portion of the cycle [18].

The BioWin ASDM model includes the three mechanisms for potential N_2O production, two mediated by AOB and one by OHO. Thus, in this study, the N_2O emissions from AOB and OHO were estimated, linking emissions to data on observable activities (Table 8). However, no N_2O measurements were carried out in this study causing uncertainty in model output results.

Table 8. N_2O production in SBR_A and SBR_B by AOB (via autotrophic denitrification), AOB (via hydroxylamine oxidation) and OHO.

	SBR_A			**SBR_B**		
	N_2O production by (kg N_2O kg $N_{removed}^{-1}$)			N_2O production (kg N_2O kg $N_{removed}^{-1}$)		
	AOB via autotrophic denitrification	AOB via hydroxylamine oxidation	OHO	AOB via autotrophic denitrification	AOB via hydroxylamine oxidation	OHO
Track study I	0.0021	0.0010	0.0009	0.0014	0.0013	0.0053
Track study II	0.0046	0.0017	0.0030	0.0036	0.0020	0.0117
Track study III	0.0075	0.0007	0.0329	0.0049	0.0013	0.1099

The overall N_2O emissions in SBR_A were estimated to be 0.117, 0.165 and 0.699 kg N per cycle, respectively, in track study I, II and III, corresponding to 0.5–3.7% of the influent N load. In SBR_B, the N_2O emission were higher and equal to 0.214, 0.368, 1.779 kg N per cycle in track study I, II and III, respectively (0.8–10% of the influent N load). Similar results have been reported by Vasilaki et al. [74] by treating an anaerobic supernatant in a nitritation-denitritation process.

AOB contributed for 78% and 68% to N_2O emission in SBR_A during Period I and II, respectively, while only for 20% in Period III. Denitrification contribution in SBR_A increased in Period III as a consequence of the higher addition of external carbon source.

In accordance with results on N_2 production, data shows that N_2O emission in SBR_B by means of heterotrophic denitrification was higher than in SBR_A, due to a higher involvement of OHO biomass with respect to anammox in nitrogen removal process. AOB contributed for 34%, 32% and 5% in N_2O emission in SBR_B in Period I, II and III, respectively.

In this study, in both SBRs, AOB denitrification played a higher role in N_2O emissions as compared to the direct N_2O production from hydroxylamine oxidation.

In order to outline a clearer picture of N_2O emission from anammox-based process further evaluations and real measurements are needed to validate modelling results.

3.8. Results Evaluation

The model has allowed to better understand the kinetic behaviour of the different bacterial groups involved in nitrogen removal. Interestingly, simulations showed that full-scale operation, contrary to what was designed, led to the development of an anammox-based process in both SBRs.

Despite the different operational strategies in terms of DO concentrations and aeration and mixing patterns adopted, in both SBRs the NOB were inhibited by the high FA concentrations, while anammox bacteria were active due to the simultaneous presence of TAN and TNN and the ability of anammox bacteria to recover from DO inhibition. The only operational condition that negatively affected the anammox activity, promoting the SPND process, was the external carbon dosage, favouring OHO in their competition for substrate (nitrite) against AAO.

The SBR_A operated in a PN/A mode was characterized by higher NLRs and a lower variability of TAN removal efficiencies compared to SBR_B as well as by a lower DO consumption and a lower external carbon dosage. All this considered, it was recommended to operate both SBRs with the same operational strategies of the SBR_A, minimizing the external carbon dosage, also in the winter period. This control strategy allows to both achieve higher and more stable nitrogen removal efficiencies and lower operational costs.

4. Conclusions

A mathematical model of anammox-based processes in SBRs treating raw mature landfill leachate has been successfully built, calibrated and validated using historical seasonal data on leachate quality, temperature, operational conditions and effluent quality. The development of this model has been carried out following a systematic guideline. The calibrated model can reproduce the behaviour of the main physical-chemical outputs (TAN, TNN, NO_3^--N and sCOD concentrations) with a good accuracy. The model allowed to understand the effects of different operating conditions (i.e: temperature, cycle phases, DO concentration, external carbon addition) on the nitrogen removal performances, demonstrating the effectiveness of the PN/A process to treat mature leachate.

Future work will be addressed in terms of the evaluation of the interaction of different factors (aeration and mixing patterns, feed COD/N, presence of inhibitors, etc.) and their impact on the process performance in regards to nitrogen removal and energy saving, making the anammox-based process in SBR easier to maintain, more cost-effective and environmentally sustainable.

Supplementary Materials: The following are available online at https://www.mdpi.com/article/10.3390/pr9081443/s1, Figure S1: an aerial photo of leachate treatment plant of Lavis, Trento, Figure S2: the schematic diagram of the leachate treatment plant, Figure S3: a line map for model calibration and validation processes, Table S1: a variation range of calibrated parameters, Table S2: a comparison of sCOD concentrations between the experimental and simulated track studies; Figure S4: a comparison of N concentrations between the experimental and simulated periods.

Author Contributions: Conceptualization, D.M., M.L.; Methodology, D.M., M.L.; Software, A.L., D.M., G.S.; Validation, A.L., D.M., M.L.; Formal analysis, A.L., D.M., M.L.; Investigation, A.L., D.M., M.L.; Resources, L.P., G.A., G.E.; Data curation, A.L., D.M., M.L.; Writing—original draft preparation, A.L., D.M., M.L., F.D.C.; writing—review and editing, L.P., G.A., G.E.; Visualization, A.L., D.M., M.L., F.D.C.; Supervision, G.A., G.E., M.L., F.D.C., G.G., W.M.; project administration, D.M., M.L., F.D.C., G.E., Funding acquisition, D.M., L.P. All authors have read and agreed to the published version of the manuscript.

Funding: This research activity has been funded by the Project "Energy efficiency of industrial products and processes", Research programme "Piano Triennale della Ricerca del Sistema Elettrico Nazionale 2019–2021" funded by the Italian Ministry of Economic Development.

Data Availability Statement: Data from this study can be made available upon request.

Acknowledgments: The authors would like to express their gratitude to the staff of ADEP—Agenzia per la Depurazione (Wastewater Treatment Agency), Autonomous Province of Trento, (Italy), DTC—Depurazione Trentino Centrale and EnviroSim Associates Ltd. for analysing samples, their technical support and constructive discussion.

Conflicts of Interest: The authors declare no conflict of interest.

References

1. Kulikowska, D.; Klimiuk, E. The effect of landfill age on municipal leachate composition. *Bioresour. Technol.* **2008**, *99*, 5981–5985. [CrossRef]
2. Brennan, R.B.; Clifford, E.; Devroedt, C.; Morrison, L.; Healy, M.G. Treatment of landfill leachate in municipal wastewater treatment plants and impacts on effluent ammonium concentrations. *J. Environ. Manag.* **2017**, *188*, 64–72. [CrossRef]
3. Ganigué, R.; Gabarró, J.; Sànchez-Melsió, A.; Ruscalleda, M.; López, H.; Vila, X.; Colprim, J.; Balaguer, M.D. Long-term operation of a partial nitritation pilot plant treating leachate with extremely high ammonium concentration prior to an anammox process. *Bioresour. Technol.* **2009**, *100*, 5624–5632. [CrossRef] [PubMed]
4. dos Santos, H.A.P.; de Castilhos Júnior, A.B.; Nadaleti, W.C.; Lourenço, V.A. Ammonia recovery from air stripping process applied to landfill leachate treatment. *Environ. Sci. Pollut. Res.* **2020**, *27*, 45108–45120. [CrossRef] [PubMed]
5. Huang, H.; Xiao, D.; Zhang, Q.; Ding, L. Removal of ammonia from landfill leachate by struvite precipitation with the use of low-cost phosphate and magnesium sources. *J. Environ. Manag.* **2014**, *145*, 191–198. [CrossRef] [PubMed]
6. Su, F.J.; Yang, S.; Huang, T.L.; Li, M.; Liu, J.R.; Yao, Y.X. Enhancement of the denitrification in low C/N condition and its mechanism by a novel isolated *Comamonas* sp. YSF15. *Environ. Pollut.* **2020**, *256*, 113294. [CrossRef]
7. Fernández, I.; Dosta, J.; Mata-Álvarez, J. A critical review of future trends and perspectives for the implementation of partial nitritation/anammox in the main line of municipal WWTPs. *Desalination Water Treat.* **2016**, *57*, 27890–27898. [CrossRef]
8. Liu, X.; Kim, M.; Nakhla, G.; Andalib, M.; Fang, Y. Partial nitrification-reactor configurations, and operational conditions: Performance analysis. *J. Environ. Chem. Eng.* **2020**, *8*, 103984. [CrossRef]
9. Rahimi, S.; Modin, O.; Mijakovic, I. Technologies for biological removal and recovery of nitrogen from wastewater. *Biotechnol. Adv.* **2020**, *43*, 107570. [CrossRef]
10. Iannacone, F.; Di Capua, F.; Granata, F.; Gargano, R.; Esposito, G. Shortcut nitrification-denitrification and biological phosphorus removal in acetate- and ethanol-fed moving bed biofilm reactors under microaerobic/aerobic conditions. *Bioresour. Technol.* **2021**, *330*, 124958. [CrossRef]
11. Di Biase, A.; Kowalski, M.S.; Devlin, T.R.; Oleszkiewicz, J.A. Moving bed biofilm reactor technology in municipal wastewater treatment: A review. *J. Environ. Manag.* **2019**, *247*, 849–866. [CrossRef] [PubMed]
12. Campo, R.; Sguanci, S.; Caffaz, S.; Mazzoli, L.; Ramazzotti, M.; Lubello, C.; Lotti, T. Efficient carbon, nitrogen and phosphorus removal from low C/N real domestic wastewater with aerobic granular sludge. *Bioresour. Technol.* **2020**, *305*, 122961. [CrossRef]
13. Yan, L.; Liu, S.; Liu, Q.; Zhang, M.; Liu, Y.; Wen, Y.; Chen, Z.; Zhang, Y.; Yang, Q. Improved performance of simultaneous nitrification and denitrification via nitrite in an oxygen-limited SBR by alternating the DO. *Bioresour. Technol.* **2019**, *275*, 153–162. [CrossRef]
14. López, H.; Puig, S.; Ganigué, R.; Ruscalleda, M.; Balaguer, M.D.; Colprim, J. Start-up and enrichment of a granular anammox SBR to treat high nitrogen load wastewaters. *J. Chem. Technol. Biotechnol.* **2008**, *83*, 1163–1169. [CrossRef]
15. Langone, M.; Ferrentino, R.; Cadonna, M.; Andreottola, A. Stoichiometric evaluation of partial nitritation, anammox and denitrification processes in a sequencing batch reactor and interpretation of online monitoring parameters. *Chemosphere* **2016**, *164*, 488–498. [CrossRef]
16. Huang, X.; Lee, P.H. Shortcut nitrification/denitrification through limited-oxygen supply with two extreme COD/N-and-ammonia active landfill leachates. *Chem. Eng. J.* **2021**, *404*, 126511. [CrossRef]
17. Zhang, S.J.; Peng, Y.Z.; Wang, S.Y.; Zheng, S.W.; Guo, J. Organic matter and concentrated nitrogen removal by shortcut nitrification and denitrification from mature municipal landfill leachate. *J. Environ. Sci.* **2007**, *19*, 647–651. [CrossRef]

18. Roots, P.; Sabba, F.; Rosenthal, A.F.; Wang, Y.; Yuan, Q.; Rieger, L.; Yang, F.; Kozak, J.A.; Zhang, H.; Wells, G.F. Integrated shortcut nitrogen and biological phosphorus removal from mainstream wastewater: Process operation and modeling. *Environ. Sci. Water Res. Technol.* **2020**, *6*, 566–580. [CrossRef]
19. Kumwimba, M.N.; Lotti, T.; Şenel, E.; Li, X.; Suanon, F. Anammox-based processes: How far have we come and what work remains? A review by bibliometric analysis. *Chemosphere* **2020**, *238*, 124627. [CrossRef]
20. Baeten, J.E.; Batstone, D.J.; Schraa, O.J.; van Loosdrecht, M.C.M.; Volcke, E.I.P. Modelling anaerobic, aerobic and partial nitritation-anammox granular sludge reactors—A review. *Water Res.* **2019**, *149*, 322–341. [CrossRef] [PubMed]
21. Wett, B. Development and implementation of a robust deammonification process. *Water Sci. Technol.* **2007**, *56*, 81–88. [CrossRef]
22. Tejera, J.; Miranda, R.; Hermosilla, D.; Urra, I.; Negro, C.; Blanco, Á. Treatment of a Mature Landfill Leachate: Comparison between Homogeneous and Heterogeneous Photo-Fenton with Different Pretreatments. *Water* **2019**, *11*, 1849. [CrossRef]
23. EnviroSim Associates LTD. Available online: http://envirosim.com/products/biowin (accessed on 3 February 2020).
24. EnviroSim Associates Ltd. *Biowin 6 Help Manual*; EnviroSim Associates Ltd: Ontario, Canada, 2019; p. 1071.
25. Rieger, L.; Gillot, S.; Gillot, S.; Langerg, G.; Ohtsuki, T.; Shaw, A.; Takács, I.; Winkler, S. *Guidelines for Using Activated Sludge Models*; IWA Scientific and Technical Report; IWA Publishing: London, UK, 2012.
26. Rice, E.W.; Baird, R.B.; Eaton, A.D. *Standard Methods for the Examination of Water and Wastewater*, 23rd ed.; APHA: Washington, DC, USA, 2017.
27. Nhat, P.T.; Biec, H.N.; Tuyet Mai, N.T.; Thanh, B.X.; Dan, N.P. Application of a partial nitritation and anammox system for the old landfill leachate treatment. *Int. Biodeterior. Biodegrad.* **2014**, *95*, 144–150. [CrossRef]
28. Wang, C.C.; Kumar, M.; Lan, C.J.; Lin, J.G. Landfill-leachate treatment by simultaneous partial nitrification, anammox and denitrification (SNAD) process. *Desalination Water Treat.* **2011**, *32*, 4–9. [CrossRef]
29. van der Lubbe, J.; van Haandel, A. *Handbook Biological Waste Water Treatment Design and Optimisation of Activated Sludge Systems*, 2nd ed.; Quist Publishing: Leidschendam, The Netherlands, 2007.
30. Taylor, A.E.; Bottomley, P.J. Nitrite production by *Nitrosomonas europaea* and *Nitrosospira* sp. AV in soils at different solution concentrations of ammonium. *Soil Biol. Biochem.* **2006**, *38*, 828–836. [CrossRef]
31. Stehr, G.; Böttcher, B.; Dittberner, P.; Rath, G.; Koops, H.P. The ammonia-oxidizing nitrifying population of the River Elbe estuary. *FEMS Microbiol. Ecol.* **1995**, *17*, 177–186. [CrossRef]
32. Laanbroek, R.; Bodelier, P.L.E.; Gerards, S. Oxygen consumption kinetics of *Nitrosomonas europaea* and *Nitrobacter hamburgensis* grown in mixed continuous cultures at different oxygen concentrations. *Arch. Microbiol.* **1994**, *161*, 156–162. [CrossRef]
33. Salem, S.; Moussa, M.S.; van Loosdrecht, M.C.M. Determination of the Decay Rate of Nitrifying Bacteria. *Biotechnol. Bioeng.* **2006**, *94*, 252–262. [CrossRef] [PubMed]
34. Munz, G.; Lubello, C.; Oleszkiewicz, J.A. Modeling the decay of ammonium oxidizing bacteria. *Water Res.* **2011**, *45*, 557–564. [CrossRef]
35. Melcer, H.; Dold, P.L.; Jones, R.M.; Bye, C.M.; Takacs, I.; Stensel, H.D.; Wilson, A.W.; Sun, P.; Bury, S. *Methods for Wastewater Characterization in Activated Sludge Modeling*; Water Environment Research Foundation: Alexandria, VA, USA, 2003.
36. Manser, R.; Gujer, W.; Siegrist, H. Decay processes of nitrifying bacteria in biological wastewater treatment systems. *Water Res.* **2006**, *40*, 2416–2426. [CrossRef] [PubMed]
37. Vadivelu, J.K.; Vel, M.; Yuan, Z.; Fux, C. Stoichiometric and Kinetic Characterisation of *Nitrobacter* in Mixed Culture by Decoupling the Growth and Energy Generation Processes. *Biotechnol. Bioeng.* **2006**, *94*, 1176–1188. [CrossRef]
38. Liu, W.; Peng, Y.; Ma, B.; Ma, L.; Jia, F.; Li, X. Dynamics of microbial activities and community structures in activated sludge under aerobic starvation. *Bioresour. Technol.* **2017**, *244*, 588–596. [CrossRef] [PubMed]
39. Scaglione, D.; Caffaz, S.; Bettazzi, E.; Lubello, C. Experimental determination of Anammox decay coefficient. *J. Chem. Technol. Biotechnol.* **2009**, *84*, 1250–1254. [CrossRef]
40. Koch, G.; Egli, K.; van der Meer, J.R.; Siegrist, H. Mathematical modeling of autotrophic denitrification in a nitrifying biofilm of a rotating biological contactor. *Water Sci. Technol.* **2000**, *41*, 191–198. [CrossRef]
41. Azari, M.; Lübken, M.; Denecke, M. Simulation of simultaneous anammox and denitrification for kinetic and physiological characterization of microbial community in a granular biofilm system. *Biochem. Eng. J.* **2017**, *127*, 206–216. [CrossRef]
42. Strous, M.; Kuenen, J.G.; Jetten, M.S.M. Key physiology of anaerobic ammonium oxidation. *Appl. Environ. Microbiol.* **1999**, *65*, 3248–3250. [CrossRef]
43. Laanbroek, H.J.; Gerards, S. Competition for limiting amounts of oxygen between grown in mixed continuous cultures. *Arch. Microbiol.* **1993**, *159*, 453–459. [CrossRef]
44. Kayee, P.; Rongsayamanont, C.; Kunapongkiti, P.; Limpiyakorn, T. Ammonia half-saturation constants of sludge with different community compositions of ammonia-oxidizing bacteria. *Environ. Eng. Res.* **2016**, *21*, 140–144. [CrossRef]
45. Anthonisen, A.C.; Loehr, R.C.; Prakasam, T.B.; Srinath, E.G. Inhibition of Nitrification by Ammonia and Nitrous Acid. *Water Pollut. Control Fed.* **1976**, *48*, 835–852.
46. Kim, D.J.; Lee, D.I.; Cha, G.C.; Keller, J. Analysis of Free Ammonia Inhibition of Nitrite Oxidizing Bacteria Using a Dissolved Oxygen Respirometer. *Environ. Eng. Res.* **2008**, *13*, 125–130. [CrossRef]
47. Jiménez, E.; Giménez, J.B.; Ruano, M.V.; Ferrer, J.; Serralta, J. Effect of pH and nitrite concentration on nitrite oxidation rate. *Bioresour. Technol.* **2011**, *102*, 8741–8747. [CrossRef] [PubMed]

48. Jiménez, E.; Giménez, J.B.; Seco, A.; Ferrer, J.; Serralta, J. Effect of pH, substrate and free nitrous acid concentrations on ammonium oxidation rate. *Bioresour. Technol.* **2012**, *124*, 478–484. [CrossRef]
49. Seuntjens, D.; Carvajal-Arroyo, J.M.; Ruopp, M.; Bunse, P.; De Mulder, C.P.; Lochmatter, S.; Agrawal, S.; Boon, N.; Lackner, S.; Vlaeminck, S.E. High-resolution mapping and modeling of anammox recovery from recurrent oxygen exposure. *Water Res.* **2018**, *144*, 522–531. [CrossRef] [PubMed]
50. Oshiki, M.; Satoh, H.; Okabe, S. Ecology and physiology of anaerobic ammonium oxidizing bacteria. *Environ. Microbiol.* **2016**, *18*, 2784–2796. [CrossRef] [PubMed]
51. Vázquez-Padín, J.; Fernádez, I.; Figueroa, M.; Mosquera-Corral, A.; Campos, J.L.; Méndez, R. Applications of Anammox based processes to treat anaerobic digester supernatant at room temperature. *Bioresour. Technol.* **2009**, *100*, 2988–2994. [CrossRef]
52. Yan, J.; Op den Camp, H.J.M.; Jetten, M.S.M.; Hu, Y.Y.; Haaijer, S.C.M. Induced cooperation between marine nitrifiers and anaerobic ammonium-oxidizing bacteria by incremental exposure to oxygen. *Syst. Appl. Microbiol.* **2010**, *33*, 407–415. [CrossRef]
53. Yan, Y.; Wang, W.; Wu, M.; Jetten, M.S.M.; Guo, J.; Ma, J.; Wang, H.; Dai, X.; Wang, Y. Transcriptomics Uncovers the Response of Anammox Bacteria to Dissolved Oxygen Inhibition and the Subsequent Recovery Mechanism. *Environ. Sci. Technol.* **2020**, *54*, 14674–14685. [CrossRef]
54. Lotti, T.; van der Star, W.R.L.; Kleerebezem, R.; Lubello, C.; van Loosdrecht, M.C.M. The effect of nitrite inhibition on the anammox process. *Water Res.* **2012**, *46*, 2559–2569. [CrossRef]
55. Chamchoi, N.; Nitisoravut, S.; Schmidt, J.E. Inactivation of ANAMMOX communities under concurrent operation of anaerobic ammonium oxidation (ANAMMOX) and denitrification. *Bioresour. Technol.* **2008**, *99*, 3331–3336. [CrossRef]
56. Ni, S.Q.; Ni, J.Y.; Hu, D.L.; Sung, S. Effect of organic matter on the performance of granular anammox process. *Bioresour. Technol.* **2012**, *110*, 701–705. [CrossRef]
57. Philips, S.; Laanbroek, H.J.; Verstraete, W. Origin, causes and effects of increased nitrite concentrations in aquatic environments. *Rev. Environ. Sci. Biotechnol.* **2002**, *1*, 115–141. [CrossRef]
58. Kim, J.H.; Guo, X.; Park, H.S. Comparison study of the effects of temperature and free ammonia concentration on nitrification and nitrite accumulation. *Process Biochem.* **2008**, *43*, 154–160. [CrossRef]
59. Azari, M.; Walter, U.; Rekers, V.; Gu, J.D.; Denecke, M. More than a decade of experience of landfill leachate treatment with a full-scale anammox plant combining activated sludge and activated carbon biofilm. *Chemosphere* **2017**, *174*, 117–126. [CrossRef]
60. Mozumder, M.S.I.; Picioreanu, C.; Van Loosdrecht, M.C.M.; Volcke, E.I.P. Effect of heterotrophic growth on autotrophic nitrogen removal in a granular sludge reactor. *Environ. Technol.* **2014**, *35*, 1027–1037. [CrossRef] [PubMed]
61. Kartal, B.; Kuypers, M.M.M.; Lavik, G.; Schalk, J.; Op den Camp, J.M.; Jetten, M.S.M.; Strous, M. Anammox bacteria disguised as denitrifiers: Nitrate reduction to dinitrogen gas via nitrite and ammonium. *Environ. Microbiol.* **2007**, *9*, 635–642. [CrossRef]
62. Sabba, F.; Picioreanu, C.; Boltz, J.P.; Nerenberg, R. Predicting N_2O emissions from nitrifying and denitrifying biofilms: A modeling study. *Water Sci. Technol.* **2017**, *75*, 530–538. [CrossRef]
63. Schulthess, R.V.; Gujer, W. Release of nitrous oxide (N_2O) from denitrifying activated sludge: Verification and application of a mathematical model. *Water Res.* **1996**, *30*, 521–530. [CrossRef]
64. Gejlsbjerg, B.; Frette, L.; Westermann, P. Dynamics of N_2O production from activated sludge. *Water Res.* **1998**, *32*, 2113–2121. [CrossRef]
65. Kimochi, Y.; Inamori, Y.; Furuya, N.; Ebisuno, T.; Matsumura, M. Characteristics of N_2O Emission and Nitrogen Removal at A DO Controlled Intermittent Aeration Activated Sludge Process. *Jpn. J. Water Treat. Biol.* **1998**, *34*, 1–14. [CrossRef]
66. Schalk-Otte, S.; Seviour, R.J.; Kuenen, J.G.; Jetten, M.S.M. Nitrous oxide (N_2O) production by *Alcaligenes faecalis* during feast and famine regimes. *Water Res.* **2000**, *34*, 2080–2088. [CrossRef]
67. Itokawa, H.; Hanaki, K.; Matsuo, T. Nitrous oxide production in high-loading biological nitrogen removal process under low cod/n ratio condition. *Water Res.* **2001**, *35*, 657–664. [CrossRef]
68. Zhou, Y.; Pijuan, M.; Zeng, R.J.; Yuan, Z. Free nitrous acid inhibition on nitrous oxide reduction by a denitrifying-enhanced biological phosphorus removal sludge. *Environ. Sci. Technol.* **2008**, *42*, 8260–8265. [CrossRef] [PubMed]
69. Wunderlin, P.; Mohn, J.; Joss, A.; Emmenegger, L.; Siegrist, H. Mechanisms of N_2O production in biological wastewater treatment under nitrifying and denitrifying conditions. *Water Res.* **2012**, *46*, 1027–1037. [CrossRef] [PubMed]
70. Hynes, R.K.; Knowles, R. Production of nitrous oxide by *Nitrosomonas europea*: Effects of acetyline, pH, and oxygen. *Can. J. Microbiol.* **1984**, *30*, 1397–1404. [CrossRef]
71. Bock, E.; Schmidt, I.; Stüven, R.; Zart, D. Nitrogen loss caused by denitrifying *Nitrosomonas* cells using ammonium or hydrogen as electron donors and nitrite as electron acceptor. *Arch. Microbiol.* **1995**, *163*, 16–20. [CrossRef]
72. Blum, J.M.; Jensen, M.M.; Smets, B.F. Nitrous oxide production in intermittently aerated Partial Nitritation-Anammox reactor: Oxic N_2O production dominates and relates with ammonia removal rate. *Chem. Eng. J.* **2018**, *335*, 458–466. [CrossRef]
73. Ali, M.; Rathnayake, R.M.L.D.; Zhang, L.; Ishii, S.; Kindaichi, T.; Satoh, H.; Okabe, S. Source identification of nitrous oxide emission pathways from a single-stage nitritation-anammox granular reactor. *Water Res.* **2016**, *102*, 147–157. [CrossRef]
74. Vasilaki, V.; Conca, V.; Frison, N.; Eusebi, A.L.; Fatone, F.; Katsou, E. A knowledge discovery framework to predict the N_2O emissions in the wastewater sector. *Water Res.* **2020**, *178*, 115799. [CrossRef]